Assessment of Texture Stationarity using the Asymptotic Behavior of the Empirical Mean and Variance

Rémi Blanc, Jean-Pierre da Costa, Youssef Stitou, Pierre Baylou, Christian Germain

Assessment of Texture Stationarity using the Asymptotic Behavior of the Empirical Mean and Variance

Rémy Blanc, Jean-Pierre Da Costa, Youssef Stitou, Pierre Baylou, and Christian Germain, *Member, IEEE*

***Abstract*— Given textured images considered as realizations of 2-D stochastic processes, a framework is proposed to evaluate the stationarity of their mean and variance. Existing strategies focus on the asymptotic behavior of the empirical mean and variance (respectively EM and EV), known for some types of non deterministic processes. In this paper, the theoretical asymptotic behaviors of the EM and EV are studied for large classes of second order stationary ergodic processes, in the sense of the Wold decomposition scheme, including harmonic and evanescent processes. Minimal rates of convergence for the EM and the EV are derived for these processes; they are used as criteria for assessing the stationarity of textures. The experimental estimation of the rate of convergence is achieved using a non parametric block sub-sampling method. Our framework is evaluated on synthetic processes with stationary or non stationary mean and variance and on real textures. It is shown that anomalies in the asymptotic behavior of the empirical estimators allow detecting non stationarities of the mean and variance of the processes in an objective way.**

***Index Terms*—Image Analysis, Stationarity, Texture, Wold Decomposition**

Manuscript received March 21, 2007. This work was funded in part by the regional council of Aquitaine, France, with the financial and technical support of the company Snecma Propulsion Solide, Safran Group.

R. Blanc is with the Computer Vision Laboratory, ETH-Zentrum, CH 8092 Zurich, Switzerland (e-mail: rblanc@vision.ee.ethz.ch).

J.-P. Da Costa (e-mail: jean-pierre.dacosta@ims-bordeaux.fr), Y. Stitou (e-mail: youssef.stitou@ims-bordeaux.fr), P. Baylou (e-mail: pierre.baylou @ims-bordeaux.fr) and C. Germain (christian.germain@ims-bordeaux.fr) are with the University of Bordeaux, IMS laboratory, France and with the CNRS, UMR 5218, France.

J.-P. Da Costa is the corresponding author. Phone+33-5-4000-2634; fax: +33-5-4000-6644; e-mail: jean-pierre.dacosta@ims-bordeaux.fr.

I. Introduction

MANAGING texture in image analysis tasks such as segmentation, classification or indexation generally requires the description of its statistical properties (e.g. [1][2][3][4][5]). Not only first-order but also second- and higher-order statistics have long been proved to influence texture perception and to efficiently help in machine-based texture recognition (e.g. [1][6][7]). The mean and variance of pixel intensity are first order statistics, whereas autocovariance, co-occurrences [1] or multidimensional histograms [2] can be used efficiently as texture descriptors of the second and higher order.

In many practical cases, the estimation of such statistical features is performed on one single, finite sample image and thus requires the double assumption of stationarity and ergodicity of the underlying 2-D random process. More precisely, stationarity and ergodicity must be assumed for every statistical moment of interest. For instance, on second order stationary-ergodic processes, the estimation of moments up to the second order, e.g. mean, variance and autocovariance, can be performed by spatial averages provided that a spatially infinite sample is available, which of course is illusory in practice. As a consequence, if the image is not stationary, the estimated statistical features are irrelevant and useless. A segmentation of the image into several homogeneous regions is then required to obtain relevant descriptive features, unless the features slowly evolve over the image, e.g. in presence of a deterministic trend, which would then have to be estimated and removed. On the contrary, statistical features estimated on a stationary region are representative not only of the observed image, but of any realization of its underlying random process, and can thus be used as a basis for comparing textures. For example, Stoica et al. [3][4] propose a method for measuring a distance between stationary textures using a parametric representation based on the Wold decomposition [8], which is employed in an indexing and retrieval application, but also for segmentation purposes. Taking advantage of the image stationarity, Blanc et al. [9] evaluate approximate confidence intervals for estimating the true fiber fraction of a composite material based on the observation of a single image.

Criteria employed to decide whether an image is stationary or not are often empirical and rely on visual inspection, thus introducing a high degree of subjectivity in the decision. That is the reason why, in practice, stationarity is generally presupposed. However, a few authors have proposed some objective criteria to study the stationarity and the ergodicity of textures. For instance in [10], ergodicity is assumed if the sample size is greater than the integral range, i.e. the integral of the normalized autocovariance. In such a case, the image sample can be considered as representative of the random process. The ergodicity can then be verified provided that several realizations of the 2-D image process are available, which seldom occurs in real-life image processing. In contrast, some tests of second order stationarity of spatial processes

have been proposed, which rely on the covariance structure [11], on spectral methods [12] or on the asymptotic distribution of spatial spectral estimates [13].

For a few decades, numbers of studies have dealt with the estimation of statistical moments on second order stationary-ergodic 2-D processes. For instance, various methods aim at drawing inferences for the statistical mean, by providing measures of its estimation variance and, by the way, of its uncertainty. Such methods are based either on geostatistical concepts [14][15] or on image sub-sampling, re-sampling or on block-bootstrap; see [16]–[20]. These approaches, though meant to measure the uncertainty in the estimation of statistical moments, can be used to evaluate their stationarity since the asymptotic behavior of their estimation variance closely depends on their homogeneity.

In the present paper, we deal with textured images considered as realizations of 2-D stochastic processes sampled on a regular grid and propose a framework to analyze the stationarity of their mean and variance in an objective way. The proposed strategy consists in comparing the asymptotic behavior of their estimation variance with the theoretical behaviors of standard processes in the sense of Wold's decomposition i.e. stochastic, harmonic and evanescent processes [8][4][5]. As any stationary random process can be decomposed as a sum of such processes, the established standard behaviors are used as references to discuss the assumption of stationarity.

The manuscript is organized as follows. Section 2 focuses on the empirical mean (EM) and empirical variance (EV) as estimators of the mean and variance of a spatial process. Theoretical expressions of their variance are given. In section 3, we provide the asymptotic laws of the EM and EV for second order stationary ergodic process, including harmonic and evanescent processes. In section 4, estimators of the variance of the EM and EV are proposed; their asymptotic behavior is studied on image samples generated according to Wold's decomposition. Finally, in section 5, our strategy for stationarity assessment is presented. It is applied to synthetic processes with stationary and non stationary mean and variance and to various real textures. Conclusions are then drawn and possible extensions of the method are discussed.

II. Estimation of the Mean and of the Variance of Spatial Processes

We consider a random process $Z(.)$ in d dimensions. We assume that a single realization $z(.)$ of $Z(.)$ is available. $z(.)$ is known only on a finite number N of points. In an image analysis context, the set of N points corresponds to the vertices of the regular lattice, or window W. N is also the Lebesgue measure of this set. For shorter notation, we will simply write $Z = Z(\boldsymbol{u})$ at an unspecified point $\boldsymbol{u}$, $Z_i = Z(\boldsymbol{u}_i)$ and $z_i = z(\boldsymbol{u}_i)$ respectively for the random process and for its available realization at the specific point $\boldsymbol{u}_i$.

A. Estimation of the Mean of a Spatial Process

Let $\mu(\boldsymbol{u}) = E[Z(\boldsymbol{u})]$ be the mathematical expectation (i.e. the mean) of $Z(\boldsymbol{u})$ and $\hat{\mu}(N)$ be the sample mean computed on the spatial sample of size *N*:

$$\hat{\mu}(N) = \frac{1}{N}\sum_{i=1}^{N} z_i \,. \tag{1}$$

If $Z(.)$ is first-order stationary, $\mu(\boldsymbol{u}) = \mu$ is invariant by translation. The sample mean $\hat{\mu}(N)$ is an unbiased estimator of μ. Herein, it will also be denoted EM (Empirical Mean). Its variance can be expressed as follows:

$$\begin{aligned} Var\left(\hat{\mu}(N)\right) &= \frac{1}{N^2}\sum_{i=1}^{N}\sum_{j=1}^{N} E\left[Z_i Z_j\right] - \mu^2 \\ &= \frac{1}{N^2}\sum_{i=1}^{N}\sum_{j=1}^{N} Cov\left(Z_i, Z_j\right) \end{aligned} \,. \tag{2}$$

where $Cov\left(Z_i, Z_j\right)$ is the covariance for the two points $\boldsymbol{u}_i$ and $\boldsymbol{u}_j$, see [10].

If the Z_i are independently and identically distributed (i.i.d.), this equation reduces to the classical expression:

$$Var\left(\hat{\mu}_{iid}(N)\right) = \frac{\sigma^2}{N} \,, \tag{3}$$

where σ^2 is the variance of the process.

In the non i.i.d. case, the evaluation of $Var\left(\hat{\mu}(N)\right)$ requires the knowledge of the covariance $Cov\left(Z_i, Z_j\right)$ between any pair of sites in the observation window W. For second order stationary processes, $Cov\left(Z_i, Z_j\right)$ is translation invariant:

$$Cov\left(Z_i, Z_j\right) = Cov(\boldsymbol{h}), \;\; where \; \boldsymbol{h} = \boldsymbol{u}_i - \boldsymbol{u}_j \,. \tag{4}$$

Equation 4 then yields:

$$Var\left(\hat{\mu}(N)\right) = \frac{1}{N^2}\sum_{\boldsymbol{h}} c_W(\boldsymbol{h}) Cov(\boldsymbol{h}) \,, \tag{5}$$

where $c_W(\boldsymbol{h})$ is the number of pairs of points in *W* that are separated by $\boldsymbol{h}$, also called the geometric covariogram, e.g. [22]. Under 2nd order stationarity and ergodicity, the autocovariance $Cov(\boldsymbol{h})$ can be estimated using spatial averages, thus providing an estimation of $Var\left(\hat{\mu}(N)\right)$. This approach will be discussed, later on, in section 4.

B. Estimation of the Variance of a Spatial Process

A simple estimator of the variance of the spatial process $Z(.)$ is the empirical variance:

$$\hat{\sigma}^2(N) = \frac{1}{N-1}\sum_{i=1}^{N}\left(z_i - \hat{\mu}(N)\right)^2 \,. \tag{6}$$

From now on, it will also be denoted EV (empirical variance). The calculation of the mathematical expectation and variance of this estimator is tractable and yields:

$$\begin{aligned} E\left[\hat{\sigma}^2(N)\right] &= \frac{1}{N-1}\left(NE\left[Z^2\right] - \frac{1}{N}\sum_{i,j} E\left[Z_i Z_j\right]\right) \\ &= \sigma^2 - Var\left(\hat{\mu}(N)\right) \end{aligned} \tag{7}$$

and

$$\begin{aligned} Var\left(\hat{\sigma}^2(N)\right) = \frac{1}{(N-1)^2}\Bigg(&\sum_{i,j} R_{iijj} - \frac{2}{N}\sum_{i,j,k} R_{iijk} \\ &+ \frac{1}{N^2}\sum_{i,j,k,l} R_{ijkl}\Bigg) - \left(E\left[\hat{\sigma}^2(N)\right]\right)^2 \end{aligned} \tag{8}$$

where $i, j, k, l \in \{1, \ldots, N\}$ and $R_{ijkl} = E\left[Z_i Z_j Z_k Z_l\right]$.

When the spatial realizations are i.i.d., $\hat{\sigma}^2(N)$ is unbiased and its variance tends to zero when *N* increases, provided that the moments $E[Z^4]$ and $E[Z^3]$ are finite:

$$Var\left(\hat{\sigma}^2_{iid}(N)\right) = \frac{2\sigma^4}{N-1} + \frac{1}{N}\left(E[Z^4] - 4\mu E[Z^3] - 3\sigma^4 + 3\mu^4 + 6\mu^2\sigma^2\right), \quad (9)$$

which simplifies to $2\sigma^4 (N-1)^{-1}$ in the Gaussian case.

The formula of $Var\left(\hat{\sigma}^2(N)\right)$, see (8), involves moments of the 4th order. Stationarity and ergodicity up to the 4th order are thus required to estimate such moments using spatial averages. Even then, their estimation implies the use of algorithms of high computational complexity.

III. Variance of the EM and EV: Asymptotic Behavior on Wold Processes.

A. Wold Decomposition of Stationary Random Processes

We restrict here to the case of 2-dimensional second order stationary random processes. According to Wold's decomposition [8][4][5], any such process is the sum of a purely stochastic component with an absolutely continuous spectrum, a finite number of harmonic components and a finite number of evanescent components. All harmonic and evanescent components are singular on the spectrum. In the following, we investigate the variances of the EM and EV on second order stationary processes following the Wold decomposition. More specifically, we are interested in the asymptotic behavior of these variances. We consider discrete rectangular windows W of sides L_X and L_Y. $N = L_X L_Y$ data points are thus available.

B. The Stochastic Component

In [10], it is assessed that the estimation of the mean of a stationary ergodic process is reliable when the integral range A is finite i.e. when the process exhibits weak spatial dependences:

$$A = \frac{1}{\sigma^2} \lim_{W \to \infty} \int_W Cov(\boldsymbol{h}) d\boldsymbol{h} < \infty, \quad (10)$$

where σ^2 is the variance of the process. If the covariance tends to zero as the modulus of h increases, if $A \neq 0$ and if the sample size N is much larger than A, then the variance of the EM of a stationary ergodic random process has the following asymptotic behavior:

$$Var\left(\hat{\mu}(N)\right) \sim \frac{\sigma^2 A}{N}. \quad (11)$$

Experiments using synthetic processes show that the asymptotic behavior can be observed when the image size is about a hundred times larger than the integral range A [10].

If $A = 0$, the decrease of $Var\left(\hat{\mu}(N)\right)$ is faster, see sections III.C and III.D hereafter. In the case of non deterministic stationary processes with long range dependences, i.e. infinite integral range, the decrease of the variance is slower. In such a case, the validity of the stationary ergodic assumption for the available sample can be questioned [10]. Such processes will not be considered here.

Besides, we have studied the asymptotic behavior of the variance of the EV, i.e. $Var\left(\hat{\sigma}^2(N)\right)$. Formal calculations, not reported in this manuscript, have shown that it depends on the convergence of integrals of fourth order moments. In the case of weak spatial dependences, i.e. with finite integral range, it was shown that $Var\left(\hat{\sigma}^2(N)\right)$ asymptotically

decreases as N^{-1}:

$$Var\left(\hat{\sigma}^2(N)\right) \sim \frac{\alpha}{N}, \quad \alpha \in \mathbb{R}^+. \tag{12}$$

C. The Harmonic Component

A harmonic process can be defined at any pixel (x, y) as follows:

$$Z(x,y) = a\sin\left(2\pi\left(f_X x + f_Y y\right) + \varphi\right), \tag{13}$$

where the phase φ is a real valued random variable whereas the amplitude a and the frequencies f_X and f_Y along the two axes are constant parameters. For such a harmonic process, the variance of the EM has been expressed as:

$$Var\left(\hat{\mu}(N)\right) = \frac{a^2 \sin^2\left(\pi f_X L_X\right)\sin^2\left(\pi f_Y L_Y\right)}{2\sin^2\left(\pi f_X\right)\sin^2\left(\pi f_Y\right)L_X^2 L_Y^2}, \tag{14}$$

where L_X and L_Y are the horizontal and vertical dimensions of the sample. $Var\left(\hat{\mu}(N)\right)$ thus decreases asymptotically as N^{-2} if neither f_X nor f_Y are zero.

On the contrary, if the harmonic process is vertical or horizontal, $Var\left(\hat{\mu}(N)\right)$ decreases as L_Y^{-2} (respectively L_X^{-2}). For square samples, i.e. $L_X = L_Y = N^{-1/2}$, $Var\left(\hat{\mu}(N)\right)$ thus decreases as N^{-1}.

Similar calculations lead to the variance of the EV:

$$Var\left(\hat{\sigma}^2(N)\right) = \frac{a^4 \sin^2\left(2\pi f_X L_X\right)\sin^2\left(2\pi f_Y L_Y\right)}{8\sin^2\left(2\pi f_X\right)\sin^2\left(2\pi f_Y\right)L_X^2 L_Y^2} + o\left(\frac{1}{L_X^2 L_Y^2}\right) \tag{15}$$

which asymptotically decreases as N^{-2}.

D. The Stochastic Component

An evanescent process can be written as a composition of two orthogonal 1-D processes:

$$Z(x,y) = T\left(\alpha x + \beta y\right)\sin\left(2\pi\left(\beta x - \alpha y\right) f + \varphi\right), \tag{16}$$

where $T(.)$ is a 1-D stochastic process orthogonal to the direction of the 1-D harmonic process. f and $\theta = \tan\left(\alpha/\beta\right)$ are respectively the frequency and the direction of the harmonic part. The phase φ is a real valued random variable.

Theoretical derivations have been carried out when $\alpha = 1$, $\beta = 0$, $T(.)$ and φ are independent white noises, following respectively a normal distribution of mean μ and variance σ^2 and a uniform distribution on the interval $[0, 2\pi[$. We found the following variance of the EM:

$$Var\left(\hat{\mu}(N)\right) = \frac{\left(\sigma^2 + \mu^2\right)}{2\sin^2\left(\pi f\right)} \cdot \frac{\sin^2\left(\pi f L_Y\right)}{L_X L_Y^2}, \tag{17}$$

and the variance of the EV :

$$Var\left(\hat{\sigma}^2(N)\right) = \frac{\sigma^2\left(\sigma^2 + 2\mu^2\right)}{2L_X} + o\left(\frac{1}{L_X L_Y}\right). \tag{18}$$

Contrary to the harmonic case, the asymptotic laws do not depend on the direction θ of the process. In the case of square samples, the variances of the EM and EV thus asymptotically decrease as $N^{-3/2}$ and $N^{-1/2}$ respectively. These results were verified experimentally even in the case where *T* was a colored noise with small range dependences, i.e. an autoregressive process, see the following section.

IV. Experimental Estimation of the Variance of the EM and EV.

In this section, we propose estimators for $Var\left(\hat{\mu}(N)\right)$ and $Var\left(\hat{\sigma}^2(N)\right)$ i.e. for the variance of the EM and EV.

These estimators are then used to verify the theoretical results of section 3.

A. Estimating the variances of the EM and EV

Geostatistics-based methods

As shown by (5), the variance of the empirical mean estimator, i.e. $Var\left(\hat{\mu}(N)\right)$, can be expressed using the autocovariance. Estimating this variance is then possible provided that an estimator of the autocovariance itself is available. Geostatistics [14][15] provide the mathematical background and the tools necessary to undertake this estimation. Parametric methods are usually preferred in order to guarantee that the estimation of the autocovariance is definite positive. Such methods are based, for instance, on the least square adjustment of autocovariance models or on the maximum likelihood estimation of the parameters of the process model itself, see for instance [15][23]. However, different choices for the autocovariance model can lead to very different estimations of the variance, while the goodness-of-fit of the models remains similar.

Likewise, equation (8) provides a framework for the estimation of $Var\left(\hat{\sigma}^2(N)\right)$. However, it implies integrals of fourth order moments. Not only the estimation of such moments would be computationally expensive but it would also require the use of parametric methods in order to guarantee the integrability of the moments and the positivity of the variance. As in the case of the autocovariance, the choice of the best parametric models would not be straightforward, making such methods inappropriate for implementation.

Nonetheless, consistent non parametric estimations based on sub-sampling exist, both for the EM and the EV, as described in the subsequent section.

Sub-sampling method

Various methods based on sub-sampling, re-sampling or block bootstrap have been proposed in literature to estimate the uncertainty of statistical moments of spatial processes (e.g. [16]–[20]).

The method proposed by Sherman and Carlstein [16] consists in splitting the image sample into various sub-samples (i.e. sub-windows) v_k of size $n < N$. On each sub-sample v_k, an estimation of the statistic of interest (EM or EV) can be computed: $\hat{\mu}_k(n)$ or $\hat{\sigma}_k^2(n)$. The sample variances can then be computed from all sub-sample estimates:

$$\widehat{Var}\left(\hat{\mu}(n)\right) = \frac{1}{K-1}\sum_{k=1}^{K}\left(\hat{\mu}_k(n) - \overline{\hat{\mu}(n)}\right)^2, \tag{19}$$

$$\widehat{Var}\left(\hat{\sigma}^2(n)\right) = \frac{1}{K-1}\sum_{k=1}^{K}\left(\hat{\sigma}_k^2(n) - \overline{\hat{\sigma}^2(n)}\right)^2, \tag{20}$$

where K is the number of available sub-samples,

$$\begin{aligned}\overline{\hat{\mu}(n)} &= \frac{1}{K}\sum_{k=1}^{K}\hat{\mu}_k(n) = \mu(N)\\ \overline{\hat{\sigma}^2(n)} &= \frac{1}{K}\sum_{k=1}^{K}\hat{\sigma}_k^2(n)\end{aligned}. \tag{21}$$

For better accuracy, sub-samples can even be chosen randomly or with overlapping [22]. These estimations are known to be consistent under mixing assumptions [20]. In other words, for large n, these estimations behave like

$Var(\hat{\mu}(N))$ and $Var(\hat{\sigma}^2(N))$. Plotting $\widehat{Var}(\hat{\mu}(n))$ and $\widehat{Var}(\hat{\sigma}^2(n))$ for increasing values of $n < N$ will then allow us to verify experimentally the rates of convergence provided by theory in section III.

B. Simulations on Wold Processes

Let us now compare these experimental estimators to the theoretical results of section 3 on synthetic image samples.

The stochastic case

Experiments were carried out to check the asymptotic behaviors of $\widehat{Var}(\hat{\mu}(n))$ and $\widehat{Var}(\hat{\sigma}^2(n))$ and to compare them with those provided by theory. Fig. 1 provides one of these experiments. It involves one thousand synthetic images generated using an autoregressive process.

For each scale n, each image was partitioned into n-sized sub-samples. The EM and the EV (respectively $\hat{\mu}_k(n)$ and $\hat{\sigma}_k^2(n)$) were then computed for each sub-sample *k*. The experimental variances $\widehat{Var}(\hat{\mu}(n))$ and $\widehat{Var}(\hat{\sigma}^2(n))$, calculated over all sub-samples, were expected to follow asymptotic laws in n^{-1} (see section 3.2) for increasing sample sizes *n*. The average values of $\widehat{Var}(\hat{\mu}(n))$ and $\widehat{Var}(\hat{\sigma}^2(n))$, computed over the 1000 images, were plotted as functions of the sample size *n*. The corresponding curves are provided in Fig. 1. 95% confidence intervals (drawn from the 1000 realizations) are also specified by vertical segments.

As shown by the asymptotes (in gray), the experimental estimations (in black) appear to decrease as n^{-1} for large sample sizes as expected by the theoretical results of section 3.2. The confidence intervals also show that the greater the scale n is, the more variable the estimations of the variances are.

The harmonic case

The same kind of experiment was carried out on harmonic processes. Here, two cases were considered depending on whether the harmonic component is oblique or not. Fig. 2 shows the results obtained on synthetic images generated following an oblique harmonic process. The asymptotic behavior observed for $\widehat{Var}(\hat{\mu}(n))$ (resp. $\widehat{Var}(\hat{\sigma}^2(n))$) is plotted on the graph in the middle (resp. on the right) of fig. 2. As anticipated in equations 14 and 15, the variances $\widehat{Var}(\hat{\mu}(n))$ and $\widehat{Var}(\hat{\sigma}^2(n))$ show envelopes with an asymptotic decrease in n^{-2}. The high variability observed at high scales is noteworthy. For harmonic processes, this variability is emphasized by the presence of sines and cosines in the theoretical expressions of the variance.

Equivalent results are obtained on harmonic components with horizontal or vertical orientation. In this case, the variability is linked to one specific direction. The decreasing rate of both variance estimations is n^{-1} instead of n^{-2}. The corresponding experimental results are given in

Fig. 3.

The evanescent case

Finally, similar experiments were driven in the case of a strictly evanescent component, following the model of equation (16). The stochastic part $T(\ )$ was generated using an autoregressive process instead of the white noise used to establish the theoretical result in section III.D. Fig. 4 shows the results obtained through 1000 realizations. In spite of the difference in the nature of $T(\ )$, the observed asymptotic behaviors are similar to the foreseen theoretical results. The envelope of $\widehat{Var}\left(\hat{\mu}(n)\right)$ decreases as $n^{-3/2}$ whereas $\widehat{Var}\left(\hat{\sigma}^2(n)\right)$ decreases as $n^{-1/2}$. Besides, we remark here again that, the greater the scale n is, the wider the confidence intervals are.

C. Simulations on Wold Processes

Table 1 summarizes the asymptotic laws obtained by theory and verified experimentally on a few examples. Results are given for various types of second order stationary processes according to Wold's decomposition. It is worthwhile to mention that these results do not include non deterministic stationary processes with long range dependences, i.e. with infinite integral range [10].

In view of these standard asymptotic behaviors, as second order stationary processes can be decomposed as sums of elementary stochastic, harmonic or evanescent components [8], it is possible to discuss the likelihood of the stationarity assumption for any process. Indeed, it can be shown that the variance of the EM (respectively of the EV) decreases as fast as or faster than the slowest of the process components. Consequently, whatever the nature of the process considered, if its mean (resp. its variance) is stationary, the rate of decrease of the EM (resp. the EV) is at least N^{-1} (resp. $N^{-1/2}$). In other words, if the decrease is slower than N^{-1} (resp. $N^{-1/2}$), the mean (resp. the variance) of the process is clearly non stationary. This makes an objective criterion to reject stationarity.

V. Application to the Assessment of Texture Stationarity

In the following, we take advantage of the properties discussed in sections III and IV to propose a method to detect non-stationarities on real image data. This method will be tested both on synthetic stationary and non stationary processes and on real textures.

A. How to Assess the Stationarity

Given a spatial sample of size N, the method of Sherman and Carlstein [16] provides with an estimate of the variances of the EM and the EV at scale $n < N$. Drawing the evolution of those variances for increasing values of n allows us to verify experimentally the rates of decrease found by theory on various stationary processes. Inversely, we can expect that, for a spatial process suffering from non-stationarities, the variances of the EM and EV will show anomalies in their rate of convergence. This gives us a method to detect non-stationarities of the mean and variance

of spatial processes.

B. Illustration on Synthetic Processes

Second order stationary process

Fig. 5 shows a realization of a synthetic stationary process generated by adding a stochastic, a harmonic and an evanescent component, mutually independent. The variance of the EM reaches its asymptotic behavior and then decreases as n^{-1}. This rate of convergence was expected by theory since it corresponds to the rate of the slowest of its components i.e. the stochastic one. As for the variance of the EV, the decrease is at the rate of $n^{-1/2}$ which is consistent with the evanescent component. In this case, the stationarity of the mean and variance can not be rejected. Stationarity is plausible.

First order stationary process

We consider now a process with a stationary mean and a non-stationary variance. The image sample in Fig. 6 corresponds to the zero mean stationary process of Fig. 5 modified by a multiplicative perturbation. The perturbation is a linear trend increasing from the top left corner to the bottom right corner so that the variance is minimum in the top left and maximum in the bottom right corner. $\widehat{Var}(\hat{\mu}(n))$ does not show any anomaly in the rate of decrease. Stationarity of the mean is plausible. The plot of $\widehat{Var}(\hat{\sigma}^2(n))$ decreases slower than $n^{-1/2}$, which shows that this process has a non stationary variance, and thus can not be considered as second order stationary.

Second order stationary process

Fig. 7 represents a process generated by applying an additive perturbation to a stationary stochastic process. This perturbation is a linear trend increasing from the top left corner to the bottom right corner. The first plot clearly shows that the mean is not stationary. However, the variance of the EV is not affected by the trend and appears homogeneous all over the image.

C. Illustration on Real Textures

The texture samples used in this section come from Brodatz's album [21]. The objective here is to evaluate the homogeneity of the textures by testing the stationarity of the underlying processes. We use the sub-sampling based approach proposed in section IV. The variances $\widehat{Var}(\hat{\mu}(n))$ and $\widehat{Var}(\hat{\sigma}^2(n))$ are thus plotted together with their estimated asymptotic trends.

Texture D64, shown in Fig. 8, gives the impression of a homogeneous texture. The rates of decrease of the variances do not invalidate this assumption, the mean and variance can thus be considered stationary.

Texture D57 in Fig. 9 looks stationary as well. However, under attentive observation, the top left corner appears to be slightly darker than the rest of the image. This non stationarity is clearly revealed by the variance of the EM, which decreases much slower than $n-1$ when the sample size increases. In contrast, the variance of the EV decreases

fast enough to consider that the process has a stationary variance.

Texture D11 in Fig. 10 looks quite homogeneous too. However, some dark spots are visible in the top left and bottom right corners. This non homogeneity is revealed by the variance of the EM. The variance of the EV, which decreases slower than $n^{-1/2}$, indicates that the variance is not homogeneous either. To help interpreting these results, we computed the local mean and the local variance of the image on a 101×101 square neighborhood. We then corrected the original texture, so that the mean and variance became homogeneous. First, we subtracted the local mean to the original image, leading to a mean-corrected image with a homogeneous zero mean. The image of the local variance was rescaled so that it ranged from 0.8 to 1.2. The corrected image (see Fig. 11) was finally obtained by dividing the mean-corrected image with the rescaled local variance. The analysis of the asymptotic behavior of the variances of the EM and EV on the corrected image shows that the non-stationarities of the mean and variance have been removed.

Finally, we present briefly the output of the method on a set of various natural textured images, extracted from the free online photo collection http://www.imageafter.com. The images are presented on Fig. 12, Table 2 summarizes the output of our method, which are discussed below.

The three images on the first row (a-c) are shown to present a stationary mean and variance, whereas the image on the second row are shown to present either a non stationary mean, a non stationary variance, or both. Image (f), on the bottom right corresponds to a filtered version of image (e) using the same correction as proposed above. Though this transformation changes significantly the aspect of the image, it is not powerful enough to produce a stationary texture, confirming that the non stationarity detected on image (e) is not due to simple causes such as lighting condition.

VI. Conclusions

In this paper, we dealt with textured images considered as realizations of 2-D spatial processes and investigated the empirical estimators of their mean (EM) and variance (EV). Theoretical expressions of their variances were given and their asymptotic behaviors were studied for large classes of 2nd order stationary ergodic processes, in the sense of the Wold decomposition scheme. In particular, minimal decreasing rates were provided for the variance of the EM and of the EV. Experimental non parametric estimators of these variances based on sub-sampling were proposed. They allowed verification of the theoretical results and showed to be consistent estimators of the variances of interest.

Based on the theoretical study and on the experimental estimation method, we proposed a strategy to inspect texture homogeneity. This strategy was applied to synthetic processes with controlled stationarity properties and to real textures from Brodatz's album. It was shown that anomalies in the asymptotic behavior of the estimators allowed

detecting non stationarities of the mean or of the variance of the processes which were difficult to detect perceptually in an objective way. This makes the presented non parametric method an interesting objective technique for the inspection of texture homogeneity.

Extensions of this work are under study. They concern the generalization of the approach to other second order statistics, i.e. the autocovariance, in order to propose a method for assessing the full 2nd order stationarity. We also expect to extend the theoretical results and empirical sub-sampling based estimators to the case of non scalar processes such as orientation vector fields. Possible applications concern the description of structural and stochastic textures with strong anisotropy properties.

REFERENCES

[1] R.M. Haralick, "Statistical and structural approaches to textures," *Proceeding of the IEEE*, vol. 67, no. 5, pp. 786–804, 1979.

[2] T. Ojala, K. Valkealahti, E. Oja, and M. Pietikäinen, "Texture discrimination with multi-dimensional distributions of signed gray-level differences," *Pattern Recognition*, vol. 34, no. 3, pp. 727–739, 2001.

[3] R. Stoica, J. Zerubia, and J.M. Francos, "Indexing and Retrieval in Multimedia Libraries Through Parametric Texture Modeling using the 2D Wold Decomposition," INRIA Research Report no 3594, 1998. Available online: ftp://ftp.inria.fr/INRIA/publication/publi-pdf/RR/RR-3594.pdf.

[4] R. Stoica, J. Zerubia, and J. M. Francos. "The Two-Dimensional Wold Decomposition for Segmentation and Indexing in Image Libraries," in *Proceedings of ICASSP*, Seattle, 1998.

[5] F. Liu and R. W. Picard, "Periodicity, Directionality, and Randomness: Wold Features for Image Modelling and Retrieval," *IEEE Trans. Pattern Anal. Mach. Intell.*, vol. 18, pp. 722–733, July 1996.

[6] A. Gagalowicz, "A new method for texture fields synthesis: some applications to the study of human vision," *IEEE Trans. Pattern Anal. Mach. Intell.*, vol. 3, no. 5, pp. 520–533, 1981.

[7] B. Julesz, "Visual pattern discrimination," *IRE Transactions on Information Theory*, pp. 84–92, 1962.

[8] J. M. Francos, A. Zvi Meiri, and B. Porat, "A Unified Texture model Based on a 2-D Wold-Like Decomposition," *IEEE Trans. Signal Process.*, vol. 41, pp. 2665–2678, August 1993.

[9] R. Blanc, J.P. Da Costa, C. Germain, and P. Baylou, "Variance of the mean value estimation of a spatial process. Application to composite material images," in *Proceedings of the 6th International Conference on Stereology, Spatial Statistics and Stochastic Geometry*, Prague, Czech Republic, 2006.

[10] C. Lantuéjoul, "Ergodicity and Integral Range," *Journal of Microscopy*, vol. 161, pt 3, pp. 387–403, March 1991.

[11] S. Bose and A.O. Steinhardt, "Invariant Tests for Spatial Stationarity using Covariance Structure," *IEEE Trans. Signal Process.*, vol. 44, pp. 1523–1533, 1996.

[12] A. Ephraty, J. Tabrikian, and H. Messer, "Underwater Source Detection using a Spatial Stationarity Test," *J. Acoust. Soc. Amer.*, vol. 109, pp. 1053–1063, 2001.

[13] M. Fuentes, "A Formal Test for Nonstationarity of Spatial Stochastic Processes," *J. Multivariate Analysis*, vol. 96, pp. 30–54, 2005.

[14] G. Matheron, *Estimating and Choosing*, Springer-Verlag, Berlin, 1989.

[15] N.A. Cressie, *Statistics for Spatial Data – Revised Edition*, New York: John Wiley & Sons, 1993.

[16] M. Sherman and E. Carlstein, "Nonparametric Estimation of the Moments of a General Statistic Computed from Spatial Data," *Journal of the American Statistical Association*, vol. 89, no. 426, pp. 496–500, 1994.

[17] M. Sherman, “Variance Estimation for Statistics Computed from Spatial Lattice Data”, *Journal of the Royal Statistical Society B*, vol. 58, no. 3, pp. 509–523, 1996.

[18] M. Sherman and E. Carlstein, “Omnibus Confidence Intervals,” Texas A&M University, Dept. of Statistics, Technical Report 278, 1997. Available online: http://www.stat.tamu.edu/ftp/pub/sherman/Papers/confint4.pdf.

[19] P. Bertail, D.N. Politis, and J.P. Romano, “On Subsampling Estimators with Unknown Rate of Convergence,” *Journal of the American Statistical Association*, vol. 94, no. 446, pp. 569–579, 1999.

[20] S.N. Lahiri, M.S. Kaiser, N. Cressie, and N-J. Hsu, “Prediction of Spatial Cumulative Distribution Functions Using Subsampling,” *Journal of the American Statistical Association*, vol. 94, no. 445, pp. 86–110, 1999.

[21] P. Brodatz, *Textures: A Photographic Album for Artists and Designers*, New York: Dover, NY, 1996.

[22] J. Serra, *Image Analysis and Mathematical Morphology*, Academic Press, London, 1982.

[23] E. Todini, “Influence of Parameter Estimation Uncertainty in Kriging: Part 1, Theoretical Development,” *Hydrology and Earth System Sciences*, vol. 5, pp. 215–223, 2001.

Rémi Blanc received a diploma in telecommunications from the Ecole Nationale d'Electronique, Informatique et Radiocommunications de Bordeaux (ENSEIRB) as well as his MSc in Electrical Engineering from the University of Bordeaux, France, in 2003. He obtained his PhD degree in Image Analysis in 2007 from the University of Bordeaux.

Since February 2008, he is working as a postdoc in the Computer Vision Laboratory of the ETH, Zurich, Switzerland. His main research topics are related to the estimation of uncertainties in statistical image analysis, including texture analysis, stereology and, more recently, statistical shape models.

Jean-Pierre Da Costa graduated as an engineer in electronics, at the ENSEIRB, Bordeaux, France, in 1998. He received his MSc degree in Signal and Image Processing in 1998 and a PhD degree in 2001 from the University of Bordeaux. He is currently an assistant professor at the agricultural school (ENITAB) of the University of Bordeaux and is involved as a researcher in the IMS laboratory, CNRS, Bordeaux. His research interests cover digital image processing and its applications, specifically agricultural remote sensing and material characterization by microscopy. His investigations concern texture analysis and texture synthesis based on orientation statistics.

Youssef Stitou received his MSc degree in statistics and applied mathematics from the University of Sidi Mohamed ben Abedellah, Fes, Morocco, in 2001. He received the PhD degree in December 2006 in signal processing from the University of Bordeaux, France.

Since September 2007, he is a Postdoctoral Fellow in the IMS laboratory, CNRS, Bordeaux France. His research interests are image and multidimensional signal processing, statistical signal processing, spectral analysis, and applications in image synthesis, classification/retrieval.

Pierre Baylou received his MSc degree from the ENSEIRB, Bordeaux, France, in 1964 and his PhD degree in communication circuits from the University of Bordeaux in 1968. He has been teaching electronics, computer science and image processing at the ENSEIRB since 1966. From 1980 to 1990, he developed autonomous robots devoted to open field agriculture. In 1990, he joined the Signal and Image group of the IMS Laboratory, CNRS. His research interests include adaptive filtering and texture analysis. The main application fields are seismic data understanding and material image analysis.

Christian Germain (M’93) received his MSc degree in Automatic Control and Signal Processing in 1993 and a PhD degree from the University of Bordeaux in 1997. He teaches computer science and image processing since 1984 and he is currently Professor at ENITAB, University of Bordeaux. He is carrying out research in the Signal and

Image group of the IMS Lab. His research interests include orientation estimation and texture characterisation in 2-D and 3-D images. Applications concern material characterization, Non Destructive Testing and high resolution remote sensing.

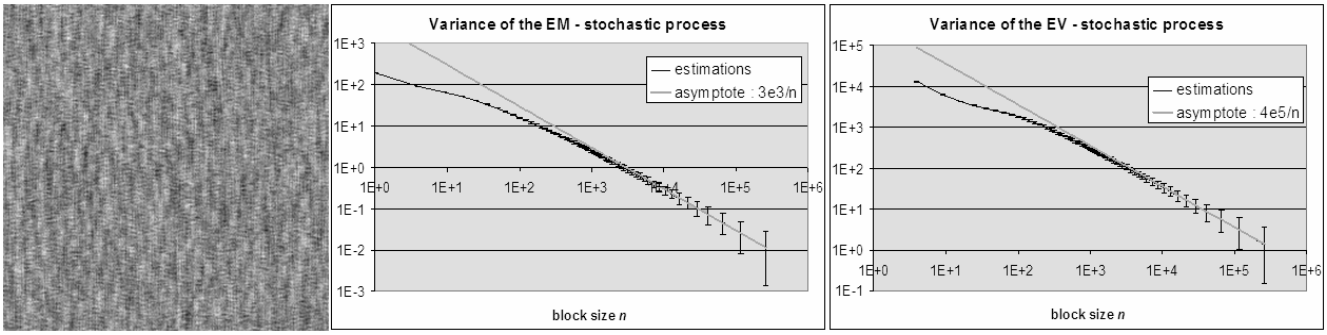

Fig. 1 Left: sample of a purely stochastic image. Middle: theoretical asymptotic curve (in gray) and experimental variance (in black) of the EM. Right: theoretical asymptotic curve (in gray) and experimental variance (in black) of the EV. The plots are in log-log scales.

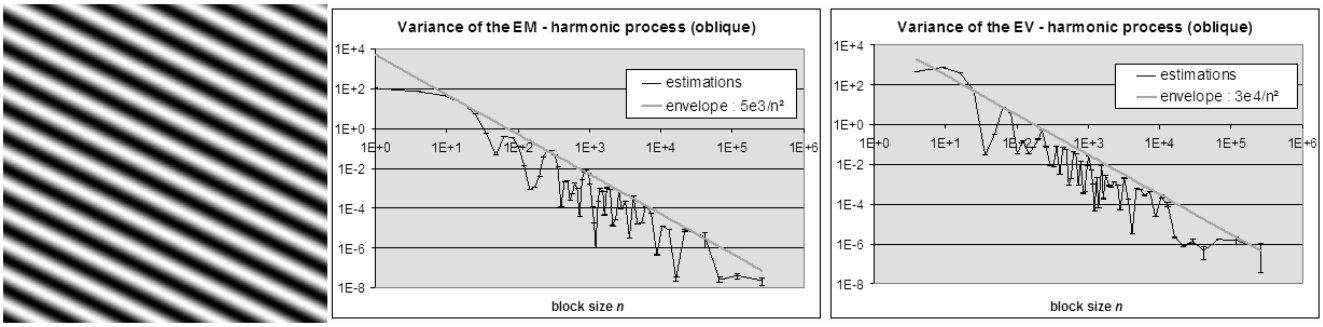

Fig. 2. Left: purely harmonic image sample with a sloped sinusoidal component. Middle: theoretical asymptotic curve (in gray) and experimental variance (in black) of the EM. Right: theoretical asymptotic curve (in gray) and experimental variance (in black) of the EV. The plots are in log-log scales.

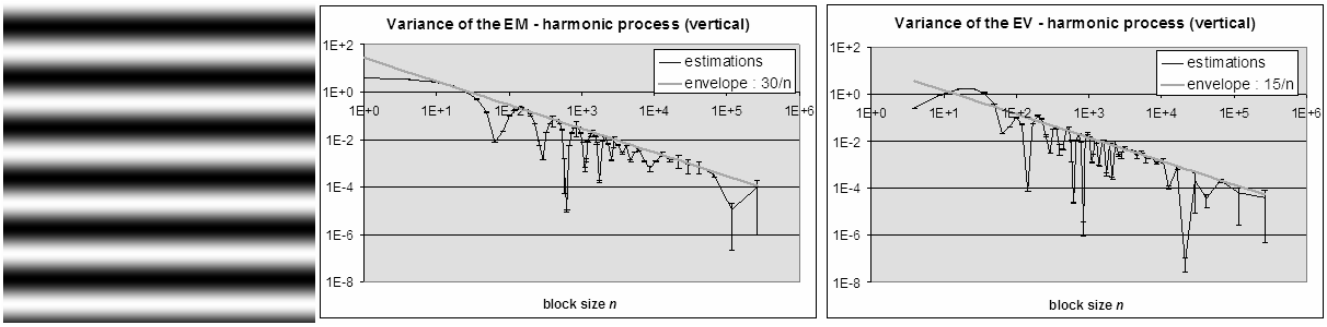

Fig. 3. Left: purely harmonic image sample with a horizontal sinusoidal component. Middle: theoretical asymptotic curve (in gray) and experimental variance (in black) of the EM. Right: theoretical asymptotic curve (in gray) and experimental variance (in black) of the EV. The plots are in log-log scale.

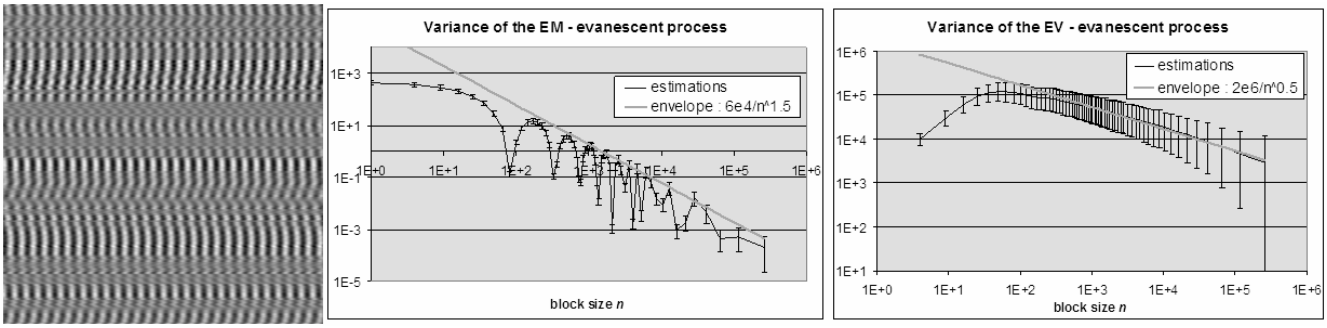

Fig. 4. Left: purely evanescent image sample. Middle: theoretical asymptotic curve (in gray) and experimental variance (in black) of the EM. Right: theoretical asymptotic curve (in gray) and experimental variance (in black) of the EV. The plots are in log-log scale.

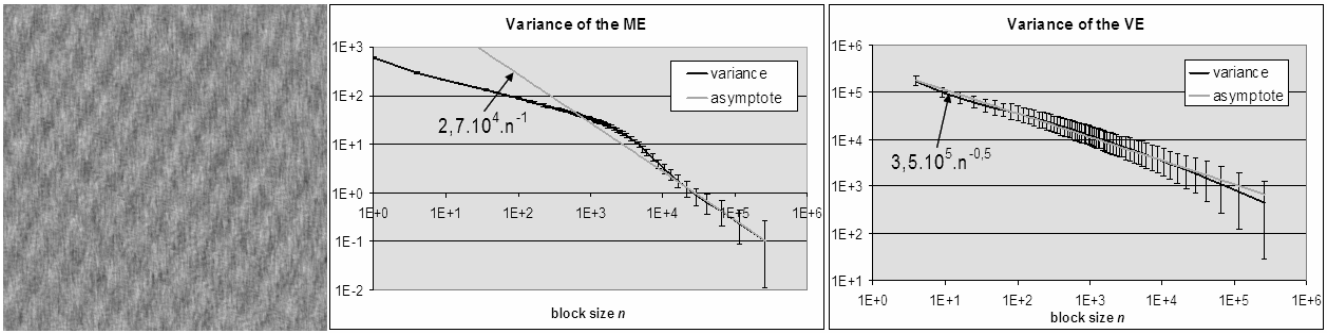

Fig. 5. Left: sample of a second order stationary process with stochastic, harmonic and evanescent components. Middle and right: plots of the estimated variances of the EM and EV versus the sub-sample scale n. The plots are in log-log scales. The curves in gray are the asymptotic trends.

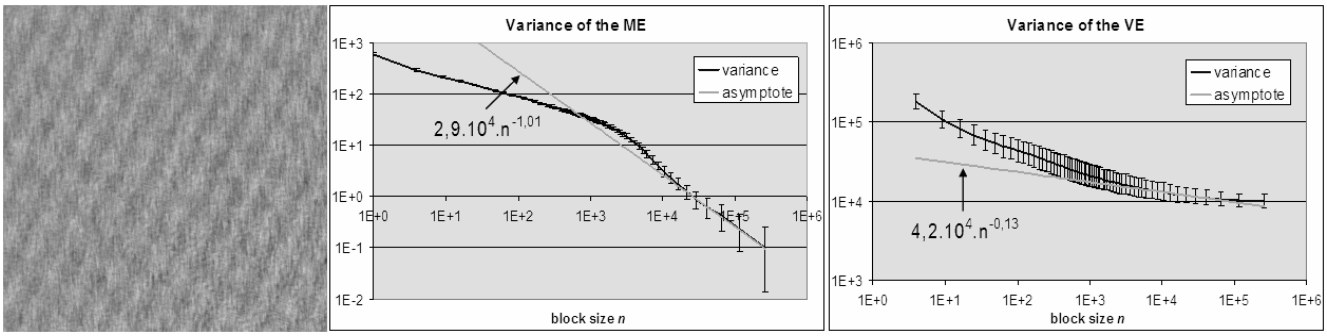

Fig. 6. Left: sample of a first order stationary process (process of Fig. 5, with non-stationary variance). Middle and right: plots of the estimated variances of the ME and VE versus the sample scale. The plots are in log-log scales. The curves in gray are the asymptotic trends of the corresponding stationary processes.

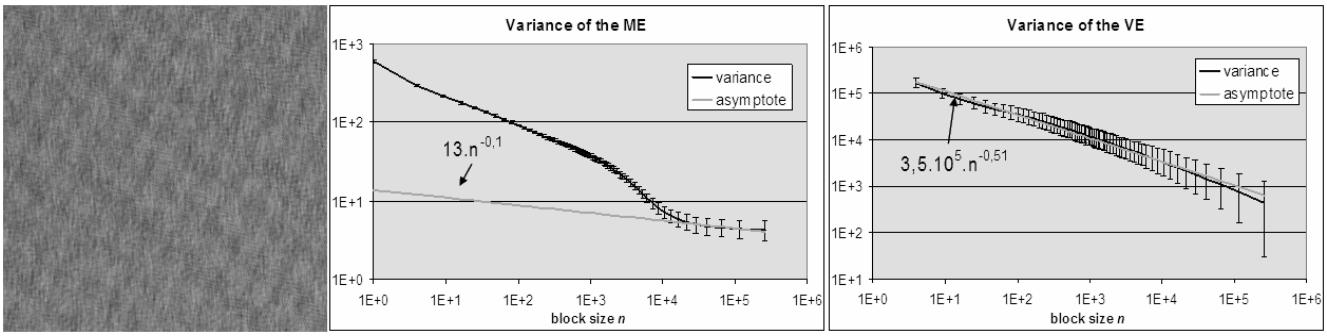

Fig. 7. Left: process sample with non-stationary mean and stationary variance (process of Fig. 5, with non-stationary mean). Middle and right: plots of the estimated variances of the EM and EV versus the sample scale. The plots are in log-log scales. The curves in gray are the asymptotic trends of the corresponding stationary processes.

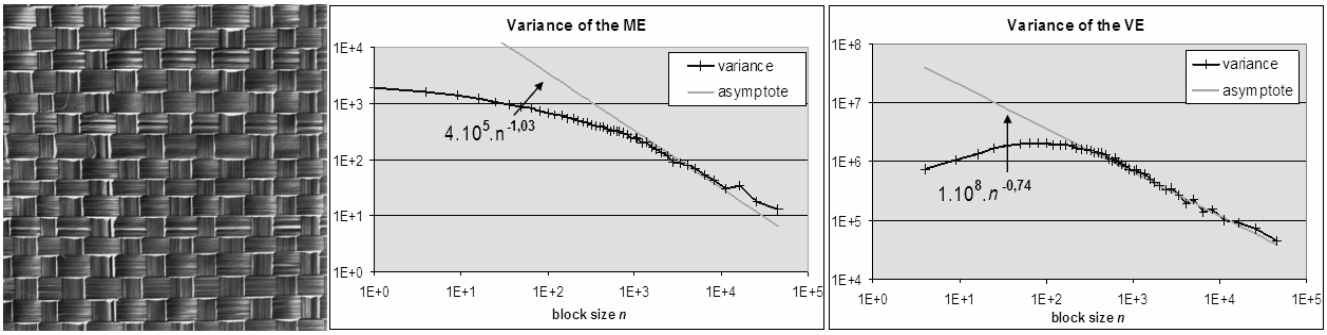

Fig. 8. Left: texture D64 from Brodatz's album. Middle and right: plots of the estimated variances of the EM and EV versus the sample scale. The plots are in log-log scales. The curves in gray are the estimated asymptotic trends.

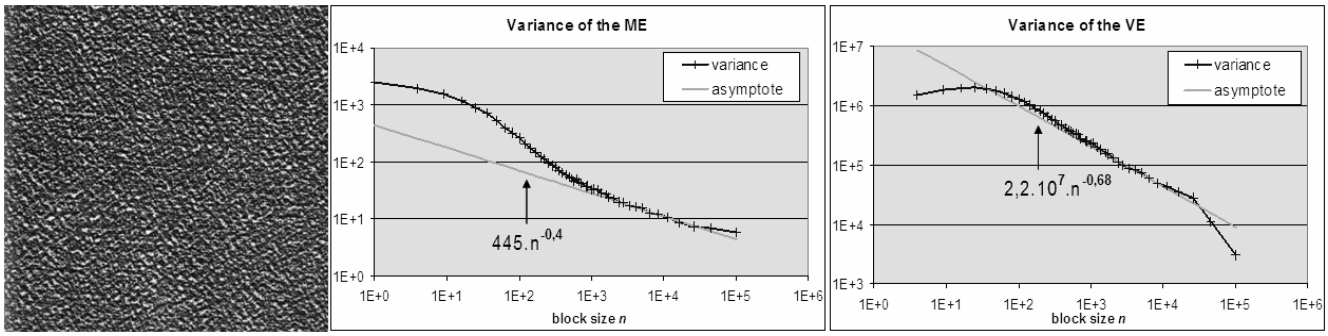

Fig. 9. Left: texture D57 from Brodatz's album. Middle and right: plots of the estimated variances of the EM and EV versus the sample scale. The plots are in log-log scales. The curves in gray are the estimated asymptotic trends.

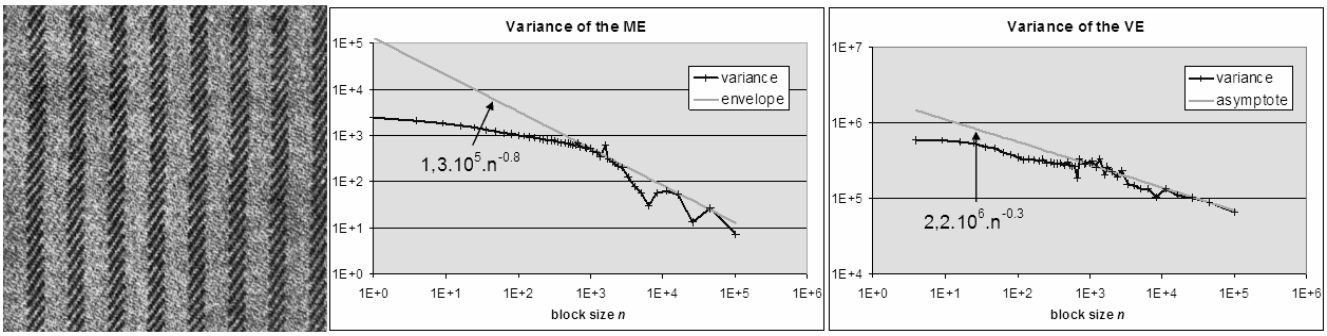

Fig. 10. Left: texture D11 from Brodatz's album. Middle and right: plots of the estimated variances of the EM and EV versus the sample scale. The plots are in log-log scales. The curves in gray are the estimated asymptotic trends. The estimated decrease rates suggest that both the mean and the variance are not homogeneous on the image.

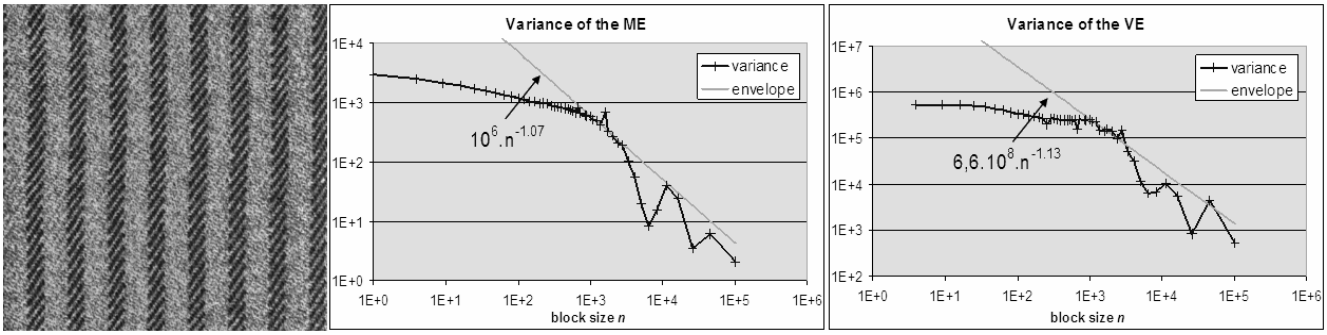

Fig. 11. Left: Corrected version of texture D11 from Brodatz's album. Middle and right: plots of the estimated variances of the EM and EV versus the sample scale. The plots are in log-log scales. The curves in gray are the estimated asymptotic trends.

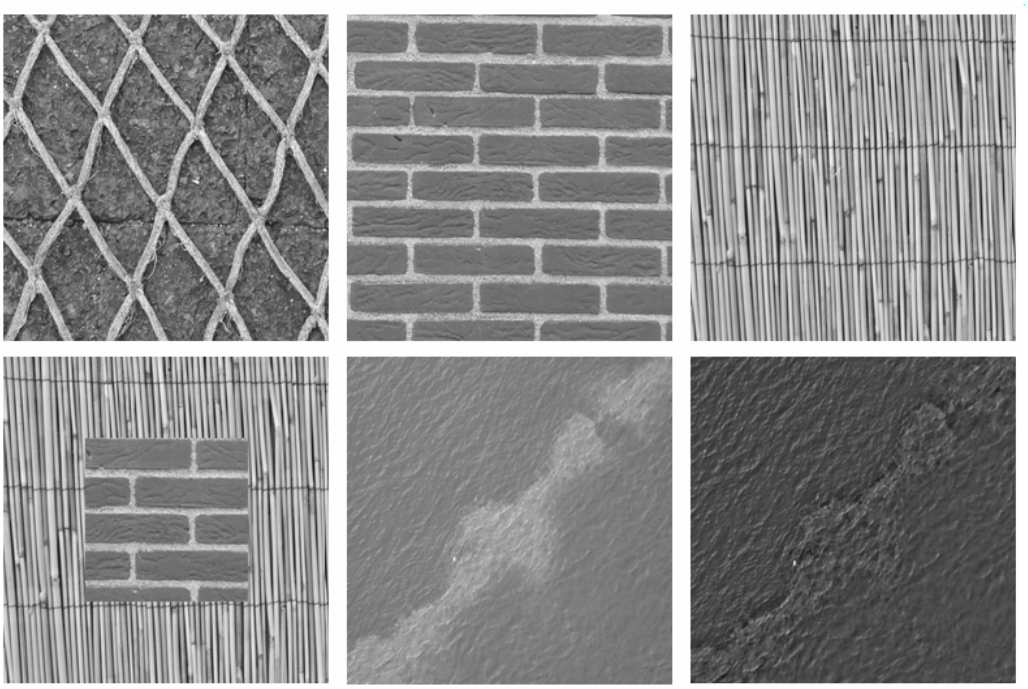

Fig. 12. Additional test images extracted or made from the free online photo collection http://www.imageafter.com. First row, from left to right: b19fabrics101 (a), b19walls317 (b), b1canefence_tr (c). Second row: compos1 (d), b9elements000 (e), b9elements000_tr (f). Images b1canefence_tr and b9elements000_tr have been transformed using the same method as for texture D11 in the previous section IV.

TABLE I

ASYMPTOTIC BEHAVIORS OF $Var\left(\hat{\mu}(N)\right)$ AND $Var\left(\hat{\sigma}^2(N)\right)$ ON SECOND ORDER STATIONARY PROCESSES FOR SQUARE IMAGE SAMPLES

Process nature	$Var\left(\hat{\mu}(N)\right)$	$Var\left(\hat{\sigma}^2(N)\right)$
Stochastic *(with finite integral range)*	N^{-1}	N^{-1}
Harmonic *(non oblique)*	N^{-1}	N^{-1}
Harmonic *(oblique)*	N^{-2}	N^{-2}
Evanescent *(magnitude with finite integral range)*	$N^{-3/2}$	$N^{-1/2}$

TABLE II

STATIONARITY ASSESSMENT FOR THE ME AND VE OF THE SIX IMAGES OF FIGURE 12.

	(a)	(b)	(c)	(d)	(e)	(f)
Slope of $\widehat{Var}\left(\hat{\mu}(n)\right)$	-1.00	-1.04	-1.00	-0.38	-0.2	-1
Stationarity of the ME	yes	yes	yes	no	no	yes
Slope of $\widehat{Var}\left(\hat{\sigma}^2(n)\right)$	-1.19	-1.1	-0.61	-0.35	+0.17	-0.14
Stationarity of the VE	yes	yes	yes	no	no	no